

Domain-Specific Risk Minimization

Yi-Fan Zhang¹, Jindong Wang², Zhang Zhang¹, Baosheng Yu³,
Liang Wang¹, Dacheng Tao³, Xing Xie²

¹Institute of Automation, Chinese Academy of Sciences

²Microsoft Research Asia, ³The University of Sydney.

August 24, 2022

Abstract

Learning a domain-invariant representation has become one of the most popular approaches for domain adaptation/generalization. In this paper, we show that the invariant representation may not be sufficient to guarantee a good generalization, where the **labeling function shift** should be taken into consideration. Inspired by this, we first derive a new generalization upper bound on the empirical risk that explicitly considers the labeling function shift. We then propose **Domain-specific Risk Minimization (DRM)**, which can model the distribution shifts of different domains separately and select the most appropriate one for the target domain. Extensive experiments on four popular domain generalization datasets, CMNIST, PACS, VLCS, and DomainNet, demonstrate the effectiveness of the proposed DRM for domain generalization with the following advantages: 1) it significantly outperforms competitive baselines; 2) it enables either comparable or superior accuracies on all training domains comparing to vanilla empirical risk minimization (ERM); 3) it remains very simple and efficient during training, and 4) it is complementary to invariant learning approaches.

1 Introduction

Machine learning models usually suffer from degraded performance when the testing data comes from a different distribution than the training data. To overcome the brittleness of classical Empirical Risk Minimization (ERM), domain generalization (DG) approaches have recently been proposed [20, 25], where models are trained on multiple large-scale source domains/datasets and can be deployed on unseen target domains directly without any data collection/annotation and/or model updating. Most deep learning-based DG methods seek to learn an *invariant representation* [5, 20, 25, 30], where the feature distributions among all source domains are the same. However, without accessing the data on the target domain, feature alignment can be performed only among source

Correspondence to: Yi-Fan Zhang <yifanzhang.cs@gmail.com>.

domains, which inevitably raises a question: whether the representation invariant to the source domain shift is good enough to generalize on the unseen target domain?

Some existing works seek to answer the question mentioned above. In theory, [50] considers the conditional shift in domain adaptation and shows that only learning invariant representation is insufficient. [2] extends the error bound in [50] to the DG setting. However, the proposed method in [2] ignores the conditional shift term as most existing DG methods. In this paper, we first construct a simple counterexample, where the invariant representation learned on source domains leads to large errors on all of source and target domains (please see the details of this counterexample in the next section). This counterexample shows that without considering the labeling function shifts of different domains, even a perfect domain-invariant representation among source domains may well lead to very large errors on both source and target domains. To better understand the effect of labeling function shifts for DG, we further prove a new generalization upper bound that considers labeling function shifts between source and target domains. The bound is not extended from the mentioned DA [50] theory and is proven tighter than that in [50]. Specifically, an intuitive explanation of the new generalization upper bound is as follows: *since we cannot guarantee that all labeling functions are the same, we would rather model all labeling functions and choose the most appropriate one for a good generalization during testing.*

Motivated by the proposed error bound, we introduce a shared encoder for all source domains with a group of domain-specific classifiers during training. Specifically, each domain-specific classifier is responsible for the labeling function on a specific source domain. During testing, motivated by the error bound, we further propose three test-time model selection strategies for classifier selection. The proposed method, **Domain-Specific Risk Minimization (DRM)**, aims to reduce the negative impact of domain labeling function variations and can be easily incorporated into most deep representation learning algorithms. Our main contributions in this paper are as follows:

- **A new perspective.** Through a counterexample, we show the insufficiency of invariant representations and provide a new generalization bound that explicitly considers the conditional shift between source and target domains. Our bound is shown tighter than the existing one and can build a connection to reweighting methods.
- **A new approach.** We propose a new Domain-specific Risk Minimization (DRM) method, which models all labeling functions in a domain-specific way. The proposed model structure and test-time selection strategy are orthogonal to most of existing methods that design new losses for DG.
- **Extensive experiments.** We perform extensive experiments on popular DG benchmarks showing that DRM (1) achieves very competitive generalization performance; (2) is orthogonal to other DG methods; (3) reserves very strong recognition capability on source domains, and (4) is parameter-efficient and converges even faster than

ERM thanks to the structure.

The rest of this paper is organized as follows. In Section 2, we analyze the failure cases of learning invariant representations for domain generalization, and provide a new generalization bound by explicitly taking into account label function shifts. After that, we present a domain-specific risk minimization (DRM) method in Section 3. We discuss the related work in Section 5 and the experimental results are shown in Section 4. Lastly, we conclude the paper in Section 6.

2 Preliminaries

Let $\mathcal{X}, \mathcal{Y}, \mathcal{Z}$ denote the input, output, and feature space, respectively. Let X, Y, Z denote the random variables taking values from $\mathcal{X}, \mathcal{Y}, \mathcal{Z}$, respectively. Each domain corresponds to a joint distribution $P_i(X, Y)$ with a labeling function $f_i : \mathcal{X} \rightarrow [0, 1]$ ¹. In the DG setting, we have access to a labeled training dataset that consists of several different but related training distributions (domains): $\mathcal{D} = \cup_{i=1}^K \mathcal{D}_i$, where K is the number of domains. In this paper, we focus on a deterministic setting where the output $Y = f_i(X)$ is given by a deterministic labeling function, f_i , which varies from domain to domain. Let $g : \mathcal{X} \rightarrow \mathcal{Z}$ denote the encoder/feature transformation and $h : \mathcal{Z} \rightarrow \{0, 1\}$ denote the classifier/hypothesis. The error incurred by $h \circ g$ under domain \mathcal{D}_i can be defined as $\epsilon_i(h \circ g) = \mathbb{E}_{X \sim \mathcal{D}_i} [|h \circ g(X) - f_i(X)|]$. Given f_i and h as binary classification functions, we have

$$\begin{aligned} \epsilon_i(h \circ g) &= \epsilon_i(h \circ g, f_i) = \mathbb{E}_{X \sim \mathcal{D}_i} [|h \circ g(X) - f_i(X)|] \\ &= \Pr_{X \sim \mathcal{D}_i} (h \circ g(X) \neq f_i(X)). \end{aligned} \tag{1}$$

During training, $h \circ g$ is trained using all image-label pairs from \mathcal{D} . During testing, we perform a retrieval task on the unseen target domain $\mathcal{D}_{\mathcal{T}}$ without additional model updating and we aim to minimize the error in $\mathcal{D}_{\mathcal{T}}$: $\min_{h \circ g} \epsilon_{\mathcal{T}}(h \circ g)$. This objective encodes the goal of learning a model that does not depend on spurious correlations (*e.g.*, domain-specific information): if a model makes decisions according to domain-specific information, it is natural to be brittle in an entirely distinct domain.

2.1 A Failure Case of Invariant Representation

In revealing flaws of learning invariant representations, we begin with a simple counterexample, where invariant representations fail to generalize. As shown in Fig. 1, given the following four domains: $\mathcal{D}_o \sim \mathcal{N}([-3, 3], I)$, $\mathcal{D}_g \sim \mathcal{N}([3, 3], I)$, $\mathcal{D}_r \sim \mathcal{N}([-3, -3], I)$, $\mathcal{D}_b \sim$

¹Most theories and examples in this paper considers binary classification for easy understanding and can be easily extended to multi-class classification.

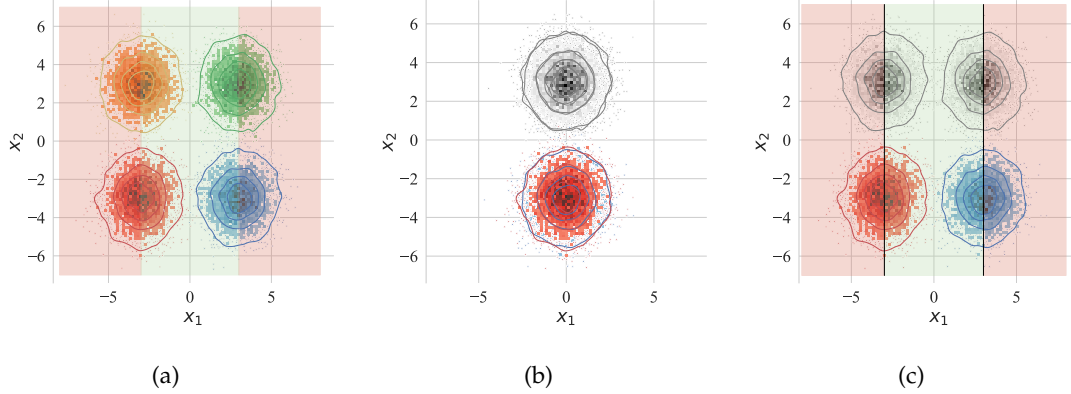


Figure 1: A failure case of invariant representations for domain generalization. (a) Four domains in different colors: **orange** ($\mu_o = [-3.0, 3.0]$), **green** ($\mu_g = [3.0, 3.0]$), **red** ($\mu_r = [-3.0, -3.0]$) and **blue** ($\mu_b = [3.0, -3.0]$). (b) Invariant representations learnt from domain \mathcal{D}_r and \mathcal{D}_b by feature transformation $g(X) = \mathbb{I}_{x_1 < 0} \cdot (x_1 + 3) + \mathbb{I}_{x_1 > 0} \cdot (x_1 - 3)$. The grey color indicates the transformed target domains. (c) The classification boundary learnt by DRM.

$\mathcal{N}([3, -3], I)$, where $X = (x_1, x_2)$ and

$$\begin{aligned}
 f_o(X) &= \begin{cases} 0, & x_1 \leq -3 \\ 1, & x_1 > -3 \end{cases}, & f_r(X) &= \begin{cases} 0, & x_1 \leq -3 \\ 1, & x_1 > -3 \end{cases}, \\
 f_g(X) &= \begin{cases} 1, & x_1 \leq 3 \\ 0, & x_1 > 3 \end{cases}, & f_b(X) &= \begin{cases} 1, & x_1 \leq 3 \\ 0, & x_1 > 3 \end{cases},
 \end{aligned} \tag{2}$$

where I indicates the identity matrix. We then have that the hypothesis $h^*(X) = 1$ iff $x_1 \in (-3, 3)$ achieves the perfect classification on all domains. Let $\mathcal{D}_r, \mathcal{D}_b$ denote source domains and $\mathcal{D}_o, \mathcal{D}_g$ denote target domains. Given a feature transformation $g(X) = \mathbb{I}_{x_1 < 0} \cdot (x_1 + 3) + \mathbb{I}_{x_1 > 0} \cdot (x_1 - 3)$ in Fig. 1 (b), the invariant representation of $\mathcal{D}_r, \mathcal{D}_b$ is learnt, which is $\mathcal{D}_{rb} = g \circ \mathcal{D}_b = g \circ \mathcal{D}_r = \mathcal{N}([0, -3], I)$. However, the labeling functions f_r of \mathcal{D}_r and f_b of \mathcal{D}_b are just the reverse such that $f_r(X) = 1 - f_b(X); \forall X \in \mathcal{D}_{rb}$. In this case, we then have $\epsilon_{rb}(h) = 1$ (see details of derivation in Appendix A.1). In other words, for any hypothesis h , the invariant representation leads to large joint errors even on all source domains, let alone unseen target domains. Therefore, given this counterexample, DG methods without considering labeling function shift are fragmentary. To make clear how labeling function shifts influence generalization performance, we prove a novel domain generalization error bound by explicitly considering the labeling function shift in the next subsection.

2.2 Domain Generalization Bound

We first provide an upper bound that is directly adapted from [6, 44].

Proposition 1. *Let \mathcal{H} be a hypothesis space and denote $\tilde{\mathcal{D}}$ as the induced distribution over feature space \mathcal{Z} for every distribution \mathcal{D} over raw space. Define \mathcal{D}_i as a source distribution over \mathcal{X} , which enables a mixture construction of source domains as $\mathcal{D}_\alpha = \sum_{i=1}^K \alpha_i \mathcal{D}_i(\cdot)$. Denote a fictitious distribution $\mathcal{D}_\mathcal{T}^\alpha = \sum_{i=1}^K \alpha_i^* \mathcal{D}_i(\cdot)$ as the convex combination of source domains which is the closest to $\mathcal{D}_\mathcal{T}$, where $\alpha_1^*, \dots, \alpha_K^* = \arg \min_{\alpha_1, \dots, \alpha_K} d_{\mathcal{H}}(\mathcal{D}_\mathcal{T}, \sum_{i=1}^K \alpha_i \mathcal{D}_i(\cdot))$. The fictitious distribution induces a feature space distribution $\tilde{\mathcal{D}}_\mathcal{T}^\alpha = \sum_{i=1}^K \alpha_i^* \tilde{\mathcal{D}}_i(\cdot)$. The following inequality holds for the risk $\epsilon_\mathcal{T}(h)$ on any unseen target domain $\mathcal{D}_\mathcal{T}$ (see appendix A.2 for detailed derivations and explanations):*

$$\epsilon_\mathcal{T}(h) \leq \lambda_\alpha + \sum_{i=1}^K \alpha_i \epsilon_i(h) + d_{\mathcal{H}}(\tilde{\mathcal{D}}_\mathcal{T}^\alpha, \tilde{\mathcal{D}}_\alpha) + d_{\mathcal{H}}(\tilde{\mathcal{D}}_\mathcal{T}, \tilde{\mathcal{D}}_\mathcal{T}^\alpha). \quad (3)$$

Many recent works on DG via learning invariant representations can get intuition from the above analysis [11, 20, 21]. Specifically, a parametric feature transformation $g : \mathcal{X} \rightarrow \mathcal{Z}$ is learned such that the induced source distributions on \mathcal{Z} are close to each other. g is called an *invariant representation w.r.t \mathcal{H}* if $d_{\mathcal{H}}(\tilde{\mathcal{D}}_i, \tilde{\mathcal{D}}_j) = 0, \forall i, j \in [1, 2, \dots, K]$. Besides, a hypothesis h over the feature space \mathcal{Z} is found to achieve small empirical errors on source domains. However, the bound also depends on the risk of the optimal hypothesis λ_α , which is usually intractable to compute for most practical hypothesis spaces and makes the bound conservative and loose in many cases. In this subsection, inspired by the counterexample, we provide a tighter upper bound for DG that considers labeling function shifts as follows.

Proposition 2. *Let $\{\mathcal{D}_i, f_i\}_{i=1}^K$ and $\mathcal{D}_\mathcal{T}, f_\mathcal{T}$ be the empirical distributions and corresponding labeling function. For any hypothesis $h \in \mathcal{H}$ and transformation g , given mixed weights $\{\alpha_i\}_{i=1}^K; \sum_{i=1}^K \alpha_i = 1, \alpha_i \geq 0$, we have:*

$$\epsilon_\mathcal{T}(h \circ g) \leq \sum_{i=1}^K \left(\mathbb{E}_{X \sim \mathcal{D}_i} \left[\alpha_i \frac{P_\mathcal{T}(X)}{P_i(X)} |h \circ g - f_i| \right] + \alpha_i \mathbb{E}_{\mathcal{D}_\mathcal{T}} [|f_i - f_\mathcal{T}|] \right). \quad (4)$$

Proof: See Appendix A.3.

The above two terms in the upper bound have natural interpretations: the first term is the weighted source errors, and the second one measures the distance between the labeling functions from the source domain and target domain. Compared to Eq.(3), Eq.(4) does not depend on λ_α , namely, the choice of the hypothesis class \mathcal{H} makes no difference. Besides, the new upper bound in Eq.(4) reflects the influence of labeling function shifts and

is independent of invariant representations. Although labeling function shift has been considered in domain adaptation error bound [3], in Appendix A.4, we show that the proposed bound is tighter. Besides, the proposed bound can supply a novel perspective for aligning labeling function shifts.

Connection between error bound (Eq. (4)) and reweighting methods. Intuitively, the density ratio stresses the importance of data sample reweighting, where data samples that are more likely from the target domain should have larger weights. Although estimating $P_{\mathcal{T}}(x)/P_i(x)$ directly is intractable, we can add constraints to the unseen target domain and get applicable formulations, which is just what distributionally robust optimization (DRO) does. Specifically, if we restrict the target domain within a f -divergence ball (such as Kullback-Leibler divergence) from the training distribution, which is also known as KL-DRO [15], then the density ratio will be converted to a reweighting term $e^{\ell/\tau^*}/\mathbb{E}[e^{\ell/\tau^*}]$ used for training, where ℓ indicates the classification error incurred by (x, y) and τ^* is a hyperparameter (See Appendix A.5 for details). Namely the reweighting term is actually an approximate estimation of the density ratio. Existing methods [22, 30, 49] use similar reweighting terms and our error bound provides a theoretical explanation for why they work well on DG.

Remark. Eq. (4) provides a new intuition on the design of DG models. Specifically, labeling functions $f_i, f_{\mathcal{T}}$ are constant and cannot be optimized. Therefore, **we focus on mixed weights α_i and $h \circ g$** . The first term will be minimized when $h \circ g$ attains low errors in source domains. The second term cannot be optimized directly, however, we can manipulate α to affect this term as follows. Given $f_{\mathcal{T}}$, if we can find the source domain \mathcal{D}_{i^*} with a labeling function f_{i^*} that minimizes $\mathbb{E}_{\mathcal{T}}[|f_{i^*} - f_{\mathcal{T}}|]$, then we have that $\alpha_i = 1$, iff $i = i^*$, otherwise 0 makes this term the minimum. As a whole algorithm, these two procedures correspond to simultaneously finding the domain \mathcal{D}_{i^*} whose labeling function is close to $f_{\mathcal{T}}$, setting $\alpha_{i^*} = 1$ and learning $h \circ g$ on \mathcal{D}_{i^*} to minimize the source error. Namely, as long as we can accurately estimate $\mathbb{E}_{\mathcal{T}}[|f_i - f_{\mathcal{T}}|]$, only one domain is required for training to minimize the error in the target domain. However, calculating $\mathbb{E}_{\mathcal{T}}[|f_{i^*} - f_{\mathcal{T}}|]$ is intractable especially when $\mathcal{D}_{\mathcal{T}}$ is unseen during training. To tackle the challenge and follow the intuition brought by Eq.(4), we propose a new Domain-Specific Risk Minimization (DRM) method for domain generalization.

3 Domain-Specific Risk Minimization

The main training and testing pipelines using the proposed Domain-Specific Risk Minimization (DRM) are shown in Figure 2.

3.1 Domain-specific labeling function

One of our main contributions is the modeling of **domain-specific labeling function**. Specifically, given K source domains, DRM utilizes a shared encoder g and a group of classifiers $\{h_i\}_{i=1}^K$ for all domains, respectively. The encoder is trained by all data sam-

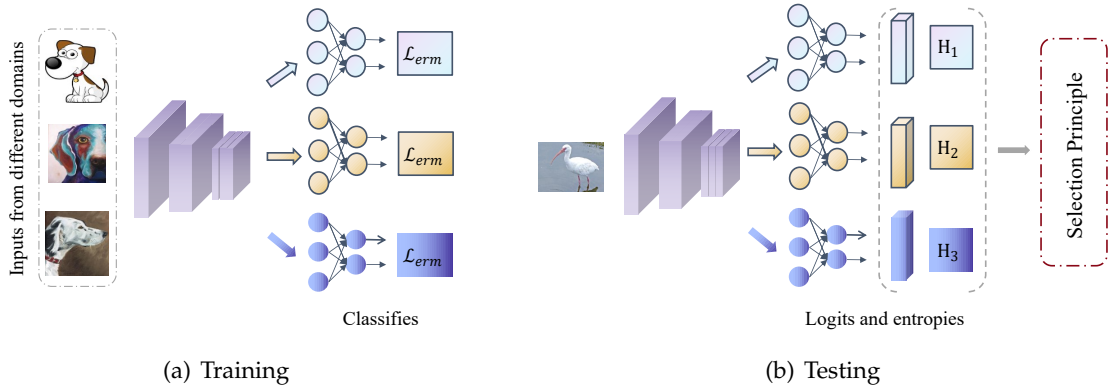


Figure 2: An illustration of the training and testing pipelines using DRM. (a) during training, it jointly optimizes an encoder shared by all domains and the specific classifiers for each individual domain. \mathcal{L}_{erm} indicates the cross-entropy loss function. (b) the new image is first classified by all classifiers and a test-time model selection strategy is applied to generate the final result.

ples while each classifier h_i is trained by using only images from the domain \mathcal{D}_i . In this way, DRM can attain 0 source error in the above-mentioned counterexample by using $g(X) = X$ and

$$h_r(X) = \begin{cases} 0 & x_1 \leq -3 \\ 1 & x_1 > -3 \end{cases}, \quad h_b(X) = \begin{cases} 1 & x_1 \leq 3 \\ 0 & x_1 > 3 \end{cases}.$$

Furthermore, the choice of g is not a matter and we can easily generalize it to other cases. For example, given $g(X) = \mathbb{I}_{x_1 < 0} \cdot (x_1 + 3) + \mathbb{I}_{x_1 > 0} \cdot (x_1 - 3)$ for invariant representation. DRM can still attain 0 source error by using

$$h_r(X) = \begin{cases} 0 & x_1 \leq 0 \\ 1 & x_1 > 0 \end{cases}, \quad h_b(X) = \begin{cases} 1 & x_1 \leq 0 \\ 0 & x_1 > 0 \end{cases}.$$

If we go back to Eq.(4), with domain-specific classifiers, we then have the bound

$$\sum_{i=1}^K \alpha_i \left(\mathbb{E}_{x \sim \mathcal{D}_i} \left[\frac{P_{\mathcal{T}}(x)}{P_i(x)} |h_i \circ g - f_i| \right] + \mathbb{E}_{\mathcal{D}_{\mathcal{T}}} [|f_i - f_{\mathcal{T}}|] \right). \quad (5)$$

Therefore, Eq.(5) shows that it is rather possible to achieve low errors on source domains by using the domain-specific classifiers than just one hypothesis h . It is also possible but not efficient to use specific $h_i \circ g_i$ for each domain. Besides, we also observe that, on the Colored MNIST dataset, it achieves the generalization accuracy 64.8% when using specific $h_i \circ g_i$, while it is 70.1% for using specific h_i . A possible reason is that a shared encoder g can be seen as an implicit regularization, which prevents the model from overfitting specific domains.

3.2 Test-time model selection.

We do not aim at a lower source error but also want to know “how to determine mixed weights α such that low target domain error can be achieved?”. As mentioned above, the second term $\alpha_i \mathbb{E}_{\mathcal{D}_T} [|f_i - f_T|]$ cannot be optimized directly, however, we can manipulate α_i to affect this term: for every test sample $x \in \mathcal{D}_T$, if we can estimate $\{H_i = |f_i(x) - f_T(x)|\}_{i=1}^K$ and choose $i^* = \arg \min \{H_i\}_{i=1}^K$. Then $\alpha_i = 1$, iff $i = i^*$, otherwise 0 makes this term the minimum and the final prediction result will be $f_{i^*} \circ g(x)$. The challenge here is estimating $\{H_i\}_{i=1}^K$. To this end, we propose three different techniques to estimate $\{H_i\}^K$ given an assumption “the learnt $h_i \circ g$ can well approximate f_i ”.

Similarity Measurement (SM). We first reformulate $\alpha_i \mathbb{E}_{\mathcal{D}_T} [|f_i - f_T|]$ as follows:

$$\begin{aligned} \alpha_i \mathbb{E}_{\mathcal{D}_T} [|f_i - f_T|] &= \alpha_i \mathbb{E}_{\mathcal{D}_T} [|f_i - \mathbb{E}_{\mathcal{D}_i} [f_i] + \mathbb{E}_{\mathcal{D}_i} [f_i] - f_T|] \\ &\leq \alpha_i (\mathbb{E}_{\mathcal{D}_T} [|f_i - \mathbb{E}_{\mathcal{D}_i} [f_i]|] + \mathbb{E}_{\mathcal{D}_T} [|\mathbb{E}_{\mathcal{D}_i} [f_i] - f_T|]), \end{aligned} \quad (6)$$

where f_T is intractable and we then focus on $\mathbb{E}_{\mathcal{D}_T} [|f_i - \mathbb{E}_{\mathcal{D}_i} [f_i]|]$, which intuitively measures the prediction difference of the given test data $x \in \mathcal{D}_T$ and the average prediction result in domain \mathcal{D}_i . However, take average of the prediction labels is meaningless² and we use $\mathbb{E}_{\mathcal{D}_T} [g - \mathbb{E}_{\mathcal{D}_i} [g]]$ to approximate this term, where we calculate the representation difference between the test sample and average representations of domain \mathcal{D}_i . Estimation H_i here is 1 minus the representation similarity between $g(x); x \in \mathcal{T}$ and domain $\mathbb{E}_{\mathcal{D}_i} [g]$. The similarity can be calculated by any distance metric such as l_p -Norm, cosine similarity, f -divergence, MMD/ \mathcal{A} distance, and we use cosine similarity (CSM) and l_2 -Norm (L2SM) in our experiments for example.

Prediction Entropy Measurement (PEM). Given the following assumption: “the more confident prediction $h_i \circ g$ makes on \mathcal{D}_T , the more similar f_i and f_T will be”. We then have, during testing, the K individual classification logits as $\{\bar{\mathbf{y}}^k\}_{k=1}^K$, where $\bar{\mathbf{y}}^k = [y_1^k, \dots, y_c^k]$, and c is the number of classes. Then, the prediction entropy of $\bar{\mathbf{y}}^k$ can be calculated as $H_k = - \sum_{i=1}^c \frac{y_i^k}{\sum_{j=1}^c y_j^k} \log \frac{y_i^k}{\sum_{j=1}^c y_j^k}$, where the entropy is used as our expected estimation. In our experiments, we find that the prediction entropy consistent with domain similarities, which is similar to SM, e.g., in the counterexample, \mathcal{D}_o is more similar to \mathcal{D}_r than to \mathcal{D}_b , hence the entropy when $X \in \mathcal{D}_o$ is classified by h_r is less than the entropy classified by h_b . In this way, Figure 1(c) shows that the learnt classification boundaries can attain 0 test errors on both the unseen target domains \mathcal{D}_o and \mathcal{D}_g .

Neural Network Measurement (NNM). To fully utilize the modeling capability of neural network, we finally propose to estimating $\alpha_i \mathbb{E}_{\mathcal{D}_T} [|f_i - f_T|]$ by NN. Specifically, during training, a domain discriminator is trained to classify which domain is each data sample from. During test, for $x \in \mathcal{D}_T$, the classification vector of the discriminator will be $\{d_i\}_{i=1}^K$, and $\{H_i = -d_i\}_{i=1}^K$ is used as the estimation.

²if all source domain has two data samples with different labels, e.g., two different one-hot labels $[0, 1]$, $[1, 0]$. Then the average prediction result of all source domains will be $[0.5, 0.5]$ and have no difference.

Model Ensembling. A one-hot mixed weight is too deterministic and cannot fully utilize all learned classifiers. **Softing mixed weights** can further boost generalization performance, *i.e.*, for ERM, we can generate the final prediction as $\sum_{k=1}^K \bar{y}_k \frac{H_k^{-\gamma}}{\sum_{i=1}^K H_i^{-\gamma}}$, where $H_k^{-\gamma}$ indicates the contribution of each classifier. We use $-\gamma$ not γ because the smaller the predicted labeling function difference between f_i and $f_{\mathcal{T}}$, the larger the contribution of f_i should be. Specifically, for $\gamma = 0$, we then have a uniform combination, *i.e.*, $\alpha_i = 1/K, \forall i \in [1, 2, \dots, K]$; for $\gamma \rightarrow \infty$, we then have a one-hot weight vector with $\alpha_i = 1$ iff $i = i^*$ otherwise 0.

Remark. By modeling domain-specific labeling functions, DRM can further reduce source errors (*i.e.*, the first term in our upper bound); For the second term, the test-time model selection strategies strategy allows us to select appropriate mixed weights and avoid directly calculating labeling function difference. Refer to Appendix Algorithm 1,2,3 for the detail of the training and test pipelines of the proposed three strategies. In the next section, we compare the proposed three strategies and PEM generally performs the best, thus we later use PEM as the default choice.

3.3 Case Studies

In this subsection, we perform case study analysis on the Colored MNIST dataset [5], where spurious correlations are manually created and can thus be a good indicator, to verify the following remarks:

- *DRM has better generalizability than invariant learning-based methods.*
- *DRM retains high accuracies on source domains and is orthogonal to invariant learning-based methods.*
- *PEM implicitly reduces prediction entropy and the entropy-based strategy performs well on finding a proper labeling function for inference.*

As shown in Table 1, ERM achieves high accuracies on training domains but below-chance accuracy on the test domain due to relying on the spurious correlations. IRM forms a tradeoff between training and testing accuracy [5]. An ERM model trained on only gray images, *i.e.*, ERM (gray), is perfectly invariant by construction, and attains a better tradeoff than IRM. The upper bound performance of invariant representations (OIM) is a hypothetical model that not only knows all spurious correlations but also has no modeling capability limit. For averaged generalization performance, DRM, without any invariance regularization, outperforms IRM by a large margin (more than 2.4%). Besides, the training accuracy attained by DRM is even higher than ERM and significantly higher than IRM and OIM. Note that DRM is complementary with invariant learning-based methods, where incorporating CORAL [36] can further boost both training and testing performances. Though the Colored MNIST dataset is a good indicator to show the model

Method	+90% ($d = 0$)		+80% ($d = 1$)		-90% ($d = 2$)		Avg	
	train	test	train	test	train	test	train	test
ERM	86.1±3.9	71.8±0.4	83.6±0.5	72.9±0.1	87.5±3.4	28.7±0.5	85.7	57.8
IRM	78.2±9.5	72.0±0.1	70.6±9.1	72.5±0.3	85.3±4.7	58.5±3.3	78	67.7
DRM	81.8±9.8	86.7±2.4	90.2±0.2	80.6±0.2	88.0±4.5	43.1±7.5	86.7	70.1
DRM+CORAL	83.4±8.6	85.3±2.3	91.6±0.7	80.7±0.2	89.4±4.9	47.2±3.6	88.1	71.1
RG	50	50	50	50	50	50	50	50
OIM	75	75	75	75	75	75	75	75
ERM (gray)	84.8±2.7	73.9±0.3	84.3±1.4	73.7±0.4	83.4±2.3	73.8±0.7	84.2	73.8

Table 1: Accuracies (%) of different methods on training/testing domains for the Colored MNIST synthetic task. OIM (optimal invariant model) and RG (random guess) are hypothetical mechanisms.

capacity for avoiding spurious correlation, these spurious correlations therein are unrealistic and utopian. Therefore, when testing on large DG benchmarks (*e.g.*, PACS, VLCS, DomainNet), ERM outperforms IRM. Different from them, DRM not only performs well on the semi-synthetic dataset but also attains state-of-the-art performance on large benchmarks.

The prediction entropy is often related to the fact that more confident predictions tend to be correct [39]. In Figure 3(a), we find that the entropy in target domain ($d = 2$) tends to be greater than the entropy in source domains, where the source domain with stronger spurious correlations ($d = 1$) also has larger entropy than easier one ($d = 0$). Fortunately, with the entropy minimization strategy, we can find the most confident classifier for a given data sample, and DRM can reduce the entropy of predictions (Figure 3(b)). To further analyze the entropy minimization strategy, we visualize the domain-classifier correlation matrix in Figure 3(c), where the entropy between the domain and its corresponding classifier is minimal, verifying the efficiency of the entropy minimization strategy. Please refer to Section 4.3 for more analysis on the domain-classifier correlation matrix.

4 Experiments

In this section, we evaluate the proposed DRM on several popular DG benchmarks. We also perform detailed ablation studies and analyses to better understand the proposed method.

4.1 Experimental Setup

We use four popular domain generalization benchmark datasets: Colored MNIST [5], Rotated MNIST [12], PACS [19], VLCS [37], and DomainNet [28]. We compare our model with ERM [38], IRM [5], Mixup [41], MLDG [18], CORAL [36], DANN [11], CDANN [21],

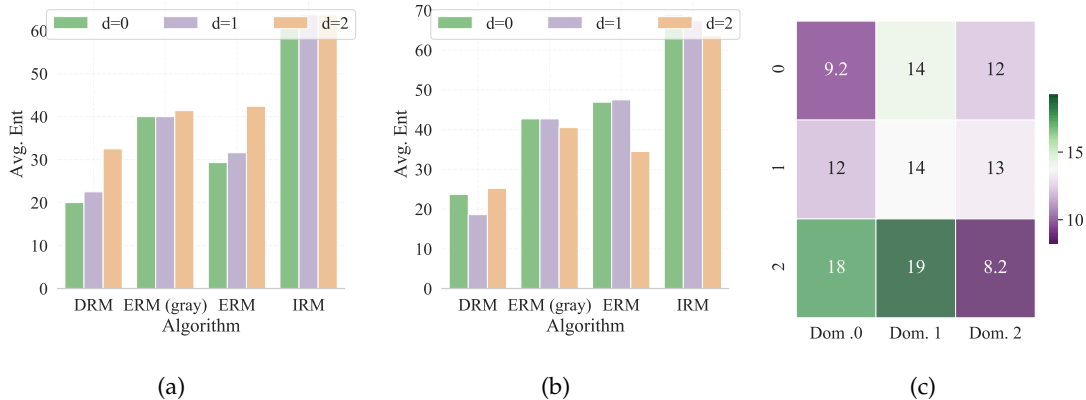


Figure 3: The entropy of different predictions. (a) Training domain $\{0, 1\}$ and testing domain $\{2\}$. (b) The average of training/testing domains $\{0, 1\}/\{2\}$, $\{0, 2\}/\{1\}$, and $\{1, 2\}/\{0\}$. (c) Domain-classifier correlation matrix, the value v_{ij} is the entropy of predictions incurred by predicting samples in domain i with classifier j . Dom. i indicates the classifier for the domain $d = i$.

MTL [8], SagNet [26], ARM [46], VREx [17], RSC [16], Fish [32], and Fishr [29]. Following [13], we use the same backbone network, ConvNet for Rotated MNIST and Colored MNIST, and ResNet-50 for the remaining datasets. For fair comparison, we use similar hyperparameters to [13] for all other datasets except the DomainNet dataset, where we observe that the proposed DRM does not converge within $5k$ iterations and we thus train it with an extra of $5k$ iterations.

4.2 Results

In this subsection, we report the performance of DRM under different generalization settings as follows.

Domain generalization. The average domain generalization results on all benchmarks are shown in Table 2. We observe consistent improvements achieved by DRM compared to existing algorithms, where the average accuracy achieved by DRM (75.6%) clearly outperforms all other methods. This result suggests that DRM has strong generalization capability on not only small semi-synthesis datasets but also large real-world benchmarks. Refer to Appendix D for generalization results on every domain of all benchmarks.

Source domain accuracy. Current DG methods do not consider keeping very good performance on source domains, while it is also of great importance in real-world applications [42]. Taking the performance on source domain into account, we then show the in-distribution performances of Rotated MNIST and DomainNet in Table 3, and VLCS and PACS in Table 4. Specifically, here we compare the classification performances (*e.g.*,

Method	Colored MNIST	Rotated MNIST	VLCS	PACS	DomainNet	Avg
IRM [5]	67.7 ± 1.2	97.5 ± 0.2	76.9 ± 0.6	84.5 ± 1.1	28.0 ± 5.1	70.9
CORAL [36]	58.6 ± 0.5	98.0 ± 0.0	77.7 ± 0.2	87.1 ± 0.5	41.8 ± 0.1	72.6
CDANN [21]	59.5 ± 2.0	97.9 ± 0.0	79.9 ± 0.2	85.8 ± 0.8	38.5 ± 0.2	72.3
ARM [46]	63.2 ± 0.7	98.1 ± 0.1	77.8 ± 0.3	85.8 ± 0.2	36.0 ± 0.2	72.2
VREx [17]	67.0 ± 1.3	97.9 ± 0.1	78.1 ± 0.2	87.2 ± 0.6	30.1 ± 3.7	72.1
RSC [16]	58.5 ± 0.5	97.6 ± 0.1	77.8 ± 0.6	86.2 ± 0.5	38.9 ± 0.6	71.8
Fish [32]	61.8 ± 0.8	97.9 ± 0.1	77.8 ± 0.6	85.8 ± 0.6	43.4 ± 0.3	73.3
Fishr [29]	68.8 ± 1.4	97.8 ± 0.1	78.2 ± 0.2	86.9 ± 0.2	41.8 ± 0.2	74.7
DRM	70.1 ± 2.0	98.1 ± 0.2	80.0 ± 0.3	87.5 ± 1.2	42.4 ± 0.1	75.6
DRM+CORAL	71.1 ± 1.7	98.3 ± 0.1	79.0 ± 2.4	87.4 ± 0.9	42.7 ± 0.1	75.7

Table 2: Out-of-distribution generalization performance.

Rotated MNIST							
Method	0	15	30	45	60	75	Avg
ERM	99.1±0.2	98.8±0.5	99.0±0.1	99.1±0.2	99.0±0.2	98.9±0.4	99.0
IRM	92.9±1.8	92.6±2.5	94.7±1.0	89.9±1.5	92.1±2.2	94.9±1.5	92.9
DRM(ours)	99.0±0.2	99.0±0.3	99.0±0.3	99.0±0.2	99.1±0.2	99.0±0.2	99.0
DomainNet							
Method	clip	info	paint	quick	real	sketch	Avg
ERM	50.4±11.4	58.3±6.2	53.4±12.6	54.6±12.7	50.8±11.0	51.9±12.6	53.2
IRM	33.4±4.1	53.2±1.4	34.0±4.1	35.1±3.4	33.0±3.8	31.5±3.1	36.7
DRM(ours)	50.1±14.3	58.3±10.4	52.5±14.7	58.1±10.3	50.2±13.2	52.1±11.5	53.6

Table 3: In-distribution performance on Rotated MNIST and DomainNet.

on PACS, when ‘P’ is chosen as the unseen target domain, the average classification performance on other domains is reported). DRM achieves comparable or even superior performance on source domains compared to ERM and beats IRM by a large margin.

Method	VLCS					PACS				
	C	L	S	V	Avg	A	C	P	S	Avg
ERM	78.2±3.3	87.8±9.0	86.3±10.2	83.3±11.6	83.9	96.7±0.3	96.4±1.5	95.3±1.2	96.3±0.1	96.2
IRM	76.9±2.9	88.2±8.9	85.3±9.8	77.3±1.0	81.9	95.9±1.6	94.2±2.5	94.3±1.0	94.5±1.8	94.7
DRM(ours)	78.5±2.9	87.2±9.2	87.3±9.0	84.0±10.9	84.3	96.9±0.3	96.4±1.3	95.2±0.9	96.1±0.6	96.2

Table 4: In-distribution performance on VLCS and PACS.

Multi-domain generalization. IRM [5] introduces specific conditions for an upper bound on the number of training environments required such that an invariant optimal model can be obtained, which stresses the importance of several training environments. In this paper, we reduce the training environments on the Rotated MNIST from five to

Rotated MNIST							
	Target domains {0, 30, 60}			Target domains {15, 45, 75}			
Method	0	30	60	15	45	75	Avg
ERM	96.0±0.3	98.8±0.4	98.7±0.1	98.8±0.3	99.1±0.1	96.7±0.3	98.0
IRM	80.9±3.2	94.7±0.9	94.3±1.3	94.3±0.8	95.5±0.5	91.1±3.1	91.8
DRM(ours)	97.1±0.2	98.8±0.2	98.9±0.3	98.8±0.1	98.8±0.0	98.1±0.7	98.4

Table 5: Generalization performance on multiple unseen target domains.

PACS dataset					
Method	A	C	P	S	Avg
Native Ensemble	81.2 ± 2.2	71.2 ± 1.2	93.7 ± 0.3	78.6 ± 1.5	81.2
CSM	83.0 ± 2.1	74.6 ± 2.5	95.6 ± 0.8	80.4 ± 1.2	83.4
L2SM	86.5 ± 2.4	77.8 ± 2.0	97.6 ± 0.4	82.8 ± 1.5	86.2
NNM	85.7 ± 1.7	84.0 ± 0.5	97.0 ± 1.6	82.1 ± 1.2	87.2
PEM	87.4 ± 2.9	83.5 ± 0.8	96.0 ± 0.5	83.0 ± 0.7	87.5

Table 6: Comparison of different test-time model selection strategies.

three. As shown in Table 5, as the number of training environment decreases, the performance of IRM fall sharply (*e.g.*, the averaged accuracy from 97.5% to 91.8%), and the performance on the most challenging domains $d = \{0, 5\}$ decline the most (94.9% \rightarrow 80.9% and 95.2% \rightarrow 91.1%). In contrast, both ERM and DRM retain high generalization performances while DRM outperforms ERM on domains $d = \{0, 5\}$.

4.3 Ablation Studies and Analysis

Comparison of test-domain selection strategies. We compare all the proposed strategies and a simple ensembling learning baseline, which use a uniform weight for classifiers ensembling. Table 6 shows that the simple ensembling learning method work poorly on all of domains, where the performance is inferior than all of existing DG methods. In contrast, ensembling learning with the weight produced by the proposed strategies achieves consistent performance gains.

Correlation matrix. From the correlation matrices, we find that: (i) The entropy of predictions between one source domain and its corresponding classifier is minimal. (ii) On the target domain, classifiers cannot attain very low entropy as they attained on the corresponding source domains. (iii) The entropy of predic-

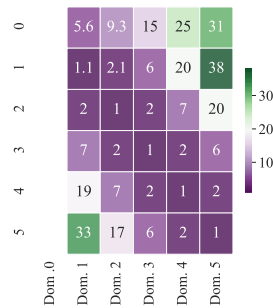


Figure 4: Domain-classifier correlation matrices on Rotated MNIST.

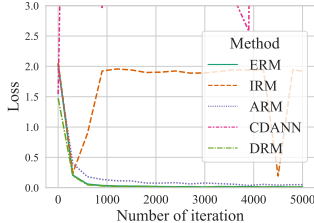
Method	Colored MNIST		Rotated MNIST		PACS	
	Time (sec)	# Params	Time (sec)	# Params	Time (sec)	# Params
ERM	71.02	0.3542M	168.32	0.3546M	2,717.5	22.4326M
IRM	101.49	0.3542M	236.8	0.3546M	2,786.3	22.4326M
CDANN	89.14	0.4492M	191.61	0.4513M	2,744.8	23.01M
ARM	161.51	0.4573M	360.69	0.4562M	6,616.9	22.5398M
FISH	137.17	0.3542M	251.76	0.3546M	23,849.5	22.4326M
DRM(ours)	83.39	0.3544M	203.15	0.3595M	2,895.1	22.46M

Table 7: Comparisons of different methods on number of parameters and training time.

tions has a certain correlation with domain similarity. For example, in Figure 4, classifier for domain $d = 1$ (with rotation angle 15°) attains the minimum entropy on the unseen target domain $d = 0$ (no rotation). As the rotation angle increases, the entropy also increases. This phenomena has also occurred in other domains. Please refer to Figure 8 for more correlation matrices.

Softing mixed weights. Figure 6 shows ablation experiments of hyper-parameter γ on three benchmarks. Different benchmarks show different preferences on γ . For easy benchmarks Rotated MNIST and Colored MNIST, softing mixed weights is needless. The reason behinds this phenomenon can be found in Figure 4, the optimal classifier for target domain 0 of Rotated MNIST is exactly the classifier 1 and the prediction entropies will increase as the rotation angle increases. Hence, selecting the most approximate classifier based on the minimum entropy selection strategy is enough to attain superior generalization results. However, prediction entropies on other larger benchmarks, *e.g.*, VLCS, are not so regular as on the Rotated MNIST. On realistic benchmarks, a mixing of classifiers can bring some improvements. Besides, normalization, which is a method to reduce classification confidence³, is also needless for semi-synthetic datasets (Rotated MNIST and Colored MNIST) and valuable for realistic benchmarks.

Model complexity. As shown in Table 7, methods that require manipulating gradients (Fish [32]) or following the meta-learning pipeline (ARM [46]) have much slower training speed compared to ERM. The proposed DRM, without the need for aligning representations [11, 21], matching gradient [32], or learning invariant representations [5, 46], has a



³Given two classification results from 2 classifiers $[2.1, 0.4, 0.5]$, $[0.3, 0.6, 0.1]$ and assume the weights are all 1. The result is $[2.4, 1.0, 0.6]$ with normalization and $[1.0, 0.73, 0.27]$ without normalization. The former is more confident than the latter.

Figure 5: Loss curves.

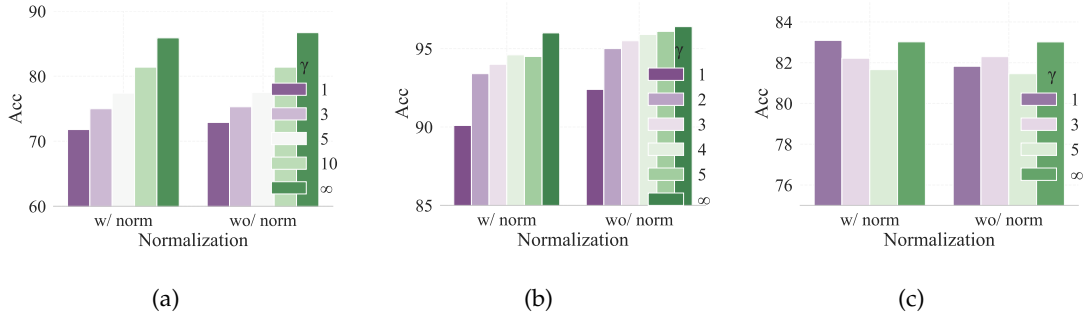


Figure 6: Different mixing weights on the (a) Colored MNIST (target domain $d = 2$) (b) Rotated MNIST (target domain $d = 0$), and (c) PACS datasets (target domain $d = 3$). Given a classification vector $\bar{y} = [y_1, y_2, \dots, y_c]$, c is the number of classes, performing normalization means that let $y_i = y_i / \sum_{j=1}^c y_j$ before mixing.

training speed that is faster than most existing DG methods especially on small datasets (ColoredMNIST and RotatedMNIST). The training speed of DRM is slower than ERM because of the need for training additional $K - 1$ classifiers. As the number of domains/classes increases or the feature dimension increases, the training time of DRM will increase accordingly, however, DRM is always comparable to ERM and much faster than Fish and ARM. For model parameters, since all classifiers in our implementation are just a linear layer, the total parameters of DRM is similar to ERM and much less than existing methods such as CDANN and ARM.

Convergence analysis. The training dynamics of DRM and several baselines on PACS dataset are shown in Figure 5, where $d = 0$ is the target domain. We can see that, due to the adversarial training nature, Domain adversarial training method (DANN) is highly unstable and hard to converge. IRM has a similar pattern yet is more stable. ARM follows a meta-learning pipeline and converges slowly. In contrast, DRM converges even faster than ERM thanks to the specific classifiers.

5 Related work

Domain adaptation and domain generalization Domain/Out-of-distribution generalization [8, 18, 21, 25, 30, 44, 48, 49] aims to learn a model that can extrapolate well in unseen environments. Representative methods like Invariant Risk Minimization (IRM) [5] and its variant [1] are recently proposed to tackle this challenge. IRM centers on the objective of extracting data representations that lead to invariant prediction across environments under a multi-environment setting. In this paper, we emphasize the importance of labeling function modeling and show that, even without an invariance strategy, the proposed

DRM can attain superior generalization capacity.

Labeling function shift and multi classifiers. Labeling function shift or conditional shift is not a novel concept and is commonly used in domain adaptation [35, 45, 50] or domain generalization [43]. There are also some studies on DG that are proposed to tackle this problem. CDANN[21] considers the scenario where both $P(X)$ and $P(Y|X)$ change across domains and propose to learn a conditional invariant neural network to minimize the discrepancy in $P(X|Y)$ across different domains. [23] explores both the conditional and label shifts in DG and aligns the conditional shift via the variational Bayesian inference. The proposed DRM is different from these studies because we want the labeling functions $P(Y|X)$ more specific to each domain rather than invariant.

Ensemble learning in domain generalization learn ensembles of multiple specific models for different source domains to improve the generalization ability, *e.g.*, domain-specific neural networks layer [10], domain-specific classifiers [40], and domain-specific batch normalization [31]. Domain-specific classifiers are also used in this work, however, empirical results show that directly ensembling multiple classifiers with a uniform weight degrades the performance and the proposed DRM can attain superior generalization result in contrast.

6 Conclusion

In this paper, we study the important problem of labeling function shifts for domain generalization theoretically and empirically. We first construct an example to show that learning an invariant representation without considering the labeling function shift is not sufficient for a good generalization. We then prove a novel upper bound for the target error, which motivates us to propose DRM to eliminate the negative effects brought by labeling function shifts. DRM achieves not only a superior generalization performance but also maintain low source errors simultaneously. We hope that our results can shed new light on the model design for domain generalization problems. One possible direction is to estimate $\alpha_i P_{\mathcal{T}}(x)/P_i(x)$ and then reweight data samples, which will be the subject of our future study. Besides, the additional parameters incurred by the multi-classifiers structure can be avoided by advanced techniques and model designs, *e.g.*, varying coefficient technique [14, 27, 47].

References

- [1] Kartik Ahuja, Karthikeyan Shanmugam, Kush Varshney, and Amit Dhurandhar. Invariant risk minimization games. In *ICML, 2020*.
- [2] Isabela Albuquerque, João Monteiro, Mohammad Darvishi, Tiago H Falk, and Ioannis Mitliagkas. Generalizing to unseen domains via distribution matching. *arXiv preprint arXiv:1911.00804*, 2019.

- [3] Isabela Albuquerque, João Monteiro, Mohammad Darvishi, Tiago H Falk, and Ioannis Mitliagkas. Generalizing to unseen domains via distribution matching. *arXiv preprint arXiv:1911.00804*, 2019.
- [4] Isabela Albuquerque, João Monteiro, Mohammad Darvishi, Tiago H Falk, and Ioannis Mitliagkas. Adversarial target-invariant representation learning for domain generalization. 2020.
- [5] Martin Arjovsky, Léon Bottou, Ishaan Gulrajani, and David Lopez-Paz. Invariant risk minimization. *arXiv preprint arXiv:1907.02893*, 2019.
- [6] Shai Ben-David, John Blitzer, Koby Crammer, and Fernando Pereira. Analysis of representations for domain adaptation. In *NIPS*, 2006.
- [7] Aharon Ben-Tal, Laurent El Ghaoui, and Arkadi Nemirovski. *Robust optimization*. Princeton university press, 2009.
- [8] Gilles Blanchard, Aniket Anand Deshmukh, Ürün Dogan, Gyemin Lee, and Clayton Scott. Domain generalization by marginal transfer learning. *J. Mach. Learn. Res.*, 2021.
- [9] Erick Delage and Yinyu Ye. Distributionally robust optimization under moment uncertainty with application to data-driven problems. *Operations research*, 2010.
- [10] Zhengming Ding and Yun Fu. Deep domain generalization with structured low-rank constraint. *IEEE Transactions on Image Processing*, 27(1):304–313, 2017.
- [11] Yaroslav Ganin, Evgeniya Ustinova, Hana Ajakan, Pascal Germain, Hugo Larochelle, François Laviolette, Mario Marchand, and Victor Lempitsky. Domain-adversarial training of neural networks. *The journal of machine learning research*, 17(1):2096–2030, 2016.
- [12] Muhammad Ghifary, W Bastiaan Kleijn, Mengjie Zhang, and David Balduzzi. Domain generalization for object recognition with multi-task autoencoders. In *ICCV*, 2015.
- [13] Ishaan Gulrajani and David Lopez-Paz. In search of lost domain generalization. In *ICLR*, 2021.
- [14] Trevor Hastie and Robert Tibshirani. Varying-coefficient models. *Journal of the Royal Statistical Society: Series B (Methodological)*, 55(4):757–779, 1993.
- [15] Zhaolin Hu and L Jeff Hong. Kullback-leibler divergence constrained distributionally robust optimization. *Available at Optimization Online*, 2013.
- [16] Zeyi Huang, Haohan Wang, Eric P Xing, and Dong Huang. Self-challenging improves cross-domain generalization. In *ECCV*, 2020.

- [17] David Krueger, Ethan Caballero, Joern-Henrik Jacobsen, Amy Zhang, Jonathan Binas, Dinghuai Zhang, Remi Le Priol, and Aaron Courville. Out-of-distribution generalization via risk extrapolation (rex). In *ICML*, 2021.
- [18] Da Li, Yongxin Yang, Yi-Zhe Song, and Timothy Hospedales. Learning to generalize: Meta-learning for domain generalization. In *AAAI*, 2018.
- [19] Da Li, Yongxin Yang, Yi-Zhe Song, and Timothy M Hospedales. Deeper, broader and artier domain generalization. In *ICCV*, 2017.
- [20] Haoliang Li, Sinno Jialin Pan, Shiqi Wang, and Alex C Kot. Domain generalization with adversarial feature learning. In *CVPR*, 2018.
- [21] Ya Li, Xinmei Tian, Mingming Gong, Yajing Liu, Tongliang Liu, Kun Zhang, and Dacheng Tao. Deep domain generalization via conditional invariant adversarial networks. In *ECCV*, 2018.
- [22] Evan Z Liu, Behzad Haghgoo, Annie S Chen, Aditi Raghunathan, Pang Wei Koh, Shiori Sagawa, Percy Liang, and Chelsea Finn. Just train twice: Improving group robustness without training group information. In *International Conference on Machine Learning (ICML)*, 2021.
- [23] Xiaofeng Liu, Bo Hu, Linghao Jin, Xu Han, Fangxu Xing, Jinsong Ouyang, Jun Lu, Georges EL Fakhri, and Jonghye Woo. Domain generalization under conditional and label shifts via variational bayesian inference. *arXiv preprint arXiv:2107.10931*, 2021.
- [24] Paul Michel, Tatsunori Hashimoto, and Graham Neubig. Modeling the second player in distributionally robust optimization. In *International Conference on Learning Representations (ICLR)*, 2021.
- [25] K. Muandet, D. Balduzzi, and B. Schölkopf. Domain generalization via invariant feature representation. In *ICML*, 2013.
- [26] Hyeonseob Nam, HyunJae Lee, Jongchan Park, Wonjun Yoon, and Donggeun Yoo. Reducing domain gap by reducing style bias. In *CVPR*, 2021.
- [27] Lizhen Nie, Mao Ye, Qiang Liu, and Dan Nicolae. Vcnet and functional targeted regularization for learning causal effects of continuous treatments. *ICLR*, 2020.
- [28] Xingchao Peng, Qinxun Bai, Xide Xia, Zijun Huang, Kate Saenko, and Bo Wang. Moment matching for multi-source domain adaptation. In *ICCV*, 2019.
- [29] Alexandre Rame, Corentin Dancette, and Matthieu Cord. Fishr: Invariant gradient variances for out-of-distribution generalization. *arXiv preprint arXiv:2109.02934*, 2021.

- [30] Shiori Sagawa, Pang Wei Koh, Tatsunori B Hashimoto, and Percy Liang. Distributionally robust neural networks for group shifts: On the importance of regularization for worst-case generalization. *arXiv preprint arXiv:1911.08731*, 2019.
- [31] Mattia Segu, Alessio Tonioni, and Federico Tombari. Batch normalization embeddings for deep domain generalization. *arXiv preprint arXiv:2011.12672*, 2020.
- [32] Yuge Shi, Jeffrey Seely, Philip Torr, Siddharth N, Awni Hannun, Nicolas Usunier, and Gabriel Synnaeve. Gradient matching for domain generalization. In *International Conference on Learning Representations*, 2022.
- [33] Aman Sinha, Hongseok Namkoong, Riccardo Volpi, and John Duchi. Certifying some distributional robustness with principled adversarial training. *arXiv preprint arXiv:1710.10571*, 2017.
- [34] Matthew Staib and Stefanie Jegelka. Distributionally robust optimization and generalization in kernel methods. *Advances in Neural Information Processing Systems (NeurIPS)*, 2019.
- [35] Petar Stojanov, Zijian Li, Mingming Gong, Ruichu Cai, Jaime G. Carbonell, and Kun Zhang. Domain adaptation with invariant representation learning: What transformations to learn? In *NeurIPS*, 2021.
- [36] Baochen Sun and Kate Saenko. Deep coral: Correlation alignment for deep domain adaptation. In *ECCV*, 2016.
- [37] Antonio Torralba and Alexei A Efros. Unbiased look at dataset bias. In *CVPR*, 2011.
- [38] Vladimir Vapnik. *The nature of statistical learning theory*. Springer science & business media, 1999.
- [39] Dequan Wang, Evan Shelhamer, Shaoteng Liu, Bruno Olshausen, and Trevor Darrell. Tent: Fully test-time adaptation by entropy minimization. In *ICLR*, 2021.
- [40] Shujun Wang, Lequan Yu, Kang Li, Xin Yang, Chi-Wing Fu, and Pheng-Ann Heng. Dofe: Domain-oriented feature embedding for generalizable fundus image segmentation on unseen datasets. *IEEE Transactions on Medical Imaging*, 39(12):4237–4248, 2020.
- [41] Shen Yan, Huan Song, Nanxiang Li, Lincan Zou, and Liu Ren. Improve unsupervised domain adaptation with mixup training. *arXiv preprint arXiv:2001.00677*, 2020.
- [42] Shiqi Yang, Yaxing Wang, Joost van de Weijer, Luis Herranz, and Shangling Jui. Generalized source-free domain adaptation. In *Proceedings of the IEEE/CVF International Conference on Computer Vision*, pages 8978–8987, 2021.

- [43] Nanyang Ye, Kaican Li, Haoyue Bai, Runpeng Yu, Lanqing Hong, Fengwei Zhou, Zhenguo Li, and Jun Zhu. Ood-bench: Quantifying and understanding two dimensions of out-of-distribution generalization. In *Proceedings of the IEEE/CVF Conference on Computer Vision and Pattern Recognition*, pages 7947–7958, 2022.
- [44] Hanlin Zhang, Yi-Fan Zhang, Weiyang Liu, Adrian Weller, Bernhard Schölkopf, and Eric P Xing. Towards principled disentanglement for domain generalization. *arXiv preprint arXiv:2111.13839*, 2021.
- [45] Kun Zhang, Bernhard Schölkopf, Krikamol Muandet, and Zhikun Wang. Domain adaptation under target and conditional shift. In *International Conference on Machine Learning*, pages 819–827. PMLR, 2013.
- [46] Marvin Zhang, Henrik Marklund, Nikita Dhawan, Abhishek Gupta, Sergey Levine, and Chelsea Finn. Adaptive risk minimization: Learning to adapt to domain shift. *NeurIPS*, 2021.
- [47] Yi-Fan Zhang, Hanlin Zhang, Zachary C Lipton, Li Erran Li, and Eric Xing. Exploring transformer backbones for heterogeneous treatment effect estimation. *arXiv*, 2022.
- [48] Yi-Fan Zhang, Zhang Zhang, Da Li, Zhen Jia, Liang Wang, and Tieniu Tan. Learning domain invariant representations for generalizable person re-identification. *arXiv preprint arXiv:2103.15890*, 2021.
- [49] YiFan Zhang, Feng Li, Zhang Zhang, Liang Wang, Dacheng Tao, and Tieniu Tan. Generalizable person re-identification without demographics, 2022.
- [50] Han Zhao, Remi Tachet Des Combes, Kun Zhang, and Geoffrey Gordon. On learning invariant representations for domain adaptation. In *ICML*. PMLR, 2019.

Domain-Specific Risk Minimization –Appendix–

A Proofs of Theoretical Statements

To complete the proofs, we begin by introducing some necessary definitions.

Definition 1. (*\mathcal{H} -divergence [6]*). Given two domain distributions $\mathcal{D}_S, \mathcal{D}_T$ over X , and a hypothesis class \mathcal{H} , the \mathcal{H} -divergence between $\mathcal{D}_S, \mathcal{D}_T$ is

$$d_{\mathcal{H}}(\mathcal{D}_S, \mathcal{D}_T) = 2 \sup_{h \in \mathcal{H}} | \mathbb{E}_{x \sim \mathcal{D}_S}[h(x) = 1] - \mathbb{E}_{x \sim \mathcal{D}_T}[h(x) = 1] |. \quad (7)$$

A.1 Derivation of constant source error

According to Eq.(1), we have

$$\begin{aligned} \epsilon_{rb}(h) &= \epsilon_r(h \circ g) + \epsilon_b(h \circ g) \\ &= \Pr_{X \sim g \circ \mathcal{D}_r}(h(X) \neq f_r(X)) + \Pr_{X \sim g \circ \mathcal{D}_b}(h(X) \neq f_b(X)) \\ &= 1 - \Pr_{X \sim \mathcal{D}_{rb}}(h(X) \neq f_b(X)) + \Pr_{X \sim \mathcal{D}_{rb}}(h(X) \neq f_b(X)) = 1 \end{aligned} \quad (8)$$

A.2 Derivation and Explanation of the Learning Bound in Eq.(3)

Let $h^* = \arg \min_{h \in \mathcal{H}} (\epsilon_{\mathcal{T}}(h) + \sum_{i=1}^K \epsilon_i(h))$, and let $\lambda_{\mathcal{T}}$ and λ_i be the errors of h^* with respect to $\mathcal{D}_{\mathcal{T}}$ and \mathcal{D}_i respectively. Notice that $\lambda_{\alpha} = \lambda_{\mathcal{T}} + \sum_{i=1}^K \lambda_i$. Similar to [6] (Theorem 1), we have

$$\begin{aligned} \epsilon_{\mathcal{T}}(h) &\leq \lambda_{\mathcal{T}} + \Pr_{\mathcal{D}_{\mathcal{T}}}[\mathcal{Z}_h \Delta \mathcal{Z}_h^*] \\ &\leq \lambda_{\mathcal{T}} + \Pr_{\mathcal{D}_{\alpha}}[\mathcal{Z}_h \Delta \mathcal{Z}_h^*] + |\Pr_{\mathcal{D}_{\alpha}}[\mathcal{Z}_h \Delta \mathcal{Z}_h^*] - \Pr_{\mathcal{D}_{\mathcal{T}}}[\mathcal{Z}_h \Delta \mathcal{Z}_h^*]| \\ &\leq \lambda_{\mathcal{T}} + \Pr_{\mathcal{D}_{\alpha}}[\mathcal{Z}_h \Delta \mathcal{Z}_h^*] + d_{\mathcal{H}}(\tilde{\mathcal{D}}_{\mathcal{T}}, \tilde{\mathcal{D}}_{\alpha}) \\ &\leq \lambda_{\mathcal{T}} + \Pr_{\mathcal{D}_{\alpha}}[\mathcal{Z}_h \Delta \mathcal{Z}_h^*] + d_{\mathcal{H}}(\tilde{\mathcal{D}}_{\mathcal{T}}^{\alpha}, \tilde{\mathcal{D}}_{\alpha}) + d_{\mathcal{H}}(\tilde{\mathcal{D}}_{\mathcal{T}}, \tilde{\mathcal{D}}_{\mathcal{T}}^{\alpha}) \\ &\leq \lambda_{\mathcal{T}} + \sum_{i=1}^K \lambda_i + \sum_{i=1}^K \alpha_i \epsilon_i(h) + d_{\mathcal{H}}(\tilde{\mathcal{D}}_{\mathcal{T}}^{\alpha}, \tilde{\mathcal{D}}_{\alpha}) + d_{\mathcal{H}}(\tilde{\mathcal{D}}_{\mathcal{T}}, \tilde{\mathcal{D}}_{\mathcal{T}}^{\alpha}) \\ &\leq \lambda_{\alpha} + \sum_{i=1}^K \alpha_i \epsilon_i(h) + d_{\mathcal{H}}(\tilde{\mathcal{D}}_{\mathcal{T}}^{\alpha}, \tilde{\mathcal{D}}_{\alpha}) + d_{\mathcal{H}}(\tilde{\mathcal{D}}_{\mathcal{T}}, \tilde{\mathcal{D}}_{\mathcal{T}}^{\alpha}), \end{aligned} \quad (9)$$

The fourth inequality holds because of the triangle inequality. We provide the explanation for our bound in Eq.(9). The second term is the empirical loss for the convex combination of all source domains. The third term corresponds to ‘‘To what extent can the convex combination of the source domain approximate the target domain’’. The minimization of the

third term requires diverse data or strong data augmentation, such that the unseen distribution lies within the convex combination of source domains. For the fourth term, the following equation holds for any two distributions D'_T, D''_T , which are the convex combinations of source domains [4]

$$d_{\mathcal{H}}[D'_T, D''_T] \leq \sum_{l=1}^K \sum_{k=1}^K \alpha_l \alpha_k d_{\mathcal{H}}[D_l, D_k] \quad (10)$$

Such an upper bound will be minimized when $d_{\mathcal{H}}[D_l, D_k] = 0, \forall l, k \in \{1, \dots, K\}$. Namely projecting the source domain data into a feature space, where the source domain labels are hard to distinguish.

A.3 Derivation the Learning Bound in Eq.(4)

Proposition 3. Let $\{\mathcal{D}_i, f_i\}_{i=1}^K$ and \mathcal{D}_T, f_T be the empirical distributions and corresponding labeling function. For any hypothesis $h \in \mathcal{H}$ and transformation \mathcal{T} , given mixed weights $\{\alpha_i\}_{i=1}^K; \sum_{i=1}^K \alpha_i = 1, \alpha_i \geq 0$, we have:

$$\epsilon_{\mathcal{T}}(h \circ g) \leq \sum_{i=1}^K \left(\mathbb{E}_{X \sim \mathcal{D}_i} \left[\alpha_i \frac{P_{\mathcal{T}}(X)}{P_i(X)} |h \circ g - f_i| \right] + \alpha_i \mathbb{E}_{\mathcal{D}_T} [|f_i - f_T|] \right)$$

Proof.

$$\begin{aligned} \epsilon_{\mathcal{T}}(h \circ g) &= \epsilon_{\mathcal{T}}(h \circ g, f_T) = \mathbb{E}_{X \sim \mathcal{D}_T} [|h \circ g(X) - f_T(X)|] \\ &= \sum_{i=1}^K \alpha_i \mathbb{E}_{X \sim \mathcal{D}_T} [|h \circ g(X) - f_T(X)|] \\ &\leq \sum_{i=1}^K \alpha_i (\mathbb{E}_{X \sim \mathcal{D}_T} [|h \circ g(X) - f_i(X) + f_i(X) - f_T(X)|]) \\ &\leq \sum_{i=1}^K \alpha_i (\mathbb{E}_{X \sim \mathcal{D}_T} [|h \circ g(X) - f_i(X)|] + \mathbb{E}_{X \sim \mathcal{D}_T} [|f_i(X) - f_T(X)|]) \\ &= \sum_{i=1}^K \alpha_i (\mathbb{E}_{\mathcal{D}_T} [|h \circ g - f_i|] + \mathbb{E}_{\mathcal{D}_T} [|f_i - f_T|]) \\ &= \sum_{i=1}^K \alpha_i \left(\int |h \circ g - f_i| P_{\mathcal{T}}(X) d_X + \mathbb{E}_{\mathcal{D}_T} [|f_i - f_T|] \right) \\ &= \sum_{i=1}^K \alpha_i \left(\int |h \circ g - f_i| P_i(X) \frac{P_{\mathcal{T}}(X)}{P_i(X)} d_X + \mathbb{E}_{\mathcal{D}_T} [|f_i - f_T|] \right) \\ &= \sum_{i=1}^K \left(\mathbb{E}_{X \sim \mathcal{D}_i} \left[\alpha_i \frac{P_{\mathcal{T}}(X)}{P_i(X)} |h \circ g - f_i| \right] + \alpha_i \mathbb{E}_{\mathcal{D}_T} [|f_i - f_T|] \right) \end{aligned}$$

□

A.4 Comparison of the proposed bound to existing bound.

Before deriving our main result, we first introduce some necessary theorems. For simplicity, given hypothesis $h, h' \in \mathcal{H}$ and label function f_S for \mathcal{D}_S , denote $\epsilon_S(h, h') = \mathbb{E}_{\tilde{\mathcal{D}}_S}[|h - h'|]$ and $\epsilon_S(h) = \epsilon_S(h, f_S) = \mathbb{E}_{\tilde{\mathcal{D}}_S}[|h - f_S|]$, we have

Theorem 1. (Lemma 4.1 and Theorem 4.1 in [3].) Given two induced distribution over feature space $\langle \tilde{\mathcal{D}}_S, f_S \rangle, \langle \tilde{\mathcal{D}}_T, f_T \rangle$ and $h \in \mathcal{H}$, we have

$$|\epsilon_S(f_S, f_T) - \epsilon_T(f_S, f_T)| \leq d_{\mathcal{H}}(\tilde{\mathcal{D}}_S, \tilde{\mathcal{D}}_T). \quad (11)$$

The error in the target domain can then be bounded by

$$\epsilon_T(h) \leq \epsilon_S(h) + d_{\mathcal{H}}(\tilde{\mathcal{D}}_S, \tilde{\mathcal{D}}_T) + \min\{\epsilon_S(f_S, f_T), \epsilon_T(f_S, f_T)\}, \quad (12)$$

where the result is mainly based on the inequality in Eq.(11).

If only two domains are considered, namely given $\langle \tilde{\mathcal{D}}_S, f_S \rangle, \langle \tilde{\mathcal{D}}_T, f_T \rangle$, recall the derivation of the proposed error bound, we have

$$\begin{aligned} \epsilon_T(h) &\leq \mathbb{E}_{\tilde{\mathcal{D}}_T}[|h - f_S|] + \mathbb{E}_{\tilde{\mathcal{D}}_T}[|f_S - f_T|] \\ &= \epsilon_T(h, f_S) + \epsilon_T(f_S, f_T) \\ &= \mathbb{E}_{X \sim \tilde{\mathcal{D}}_S} \left[\frac{P_T(X)}{P_S(X)} |h - f_S| \right] + \epsilon_T(f_S, f_T) \end{aligned} \quad (13)$$

Then we will prove that Eq.(13) is upper bounded by Eq.(12). At first, the second line in Eq.(13) is bounded by

$$\begin{aligned} \epsilon_T(h, f_S) + \epsilon_T(f_S, f_T) &\leq \epsilon_S(h, f_S) + d_{\mathcal{H}}(\tilde{\mathcal{D}}_S, \tilde{\mathcal{D}}_T) + \epsilon_T(f_S, f_T) \\ &= \epsilon_S(h) + \epsilon_T(f_S, f_T) + d_{\mathcal{H}}(\tilde{\mathcal{D}}_S, \tilde{\mathcal{D}}_T). \end{aligned} \quad (14)$$

Besides, as the density ration $\frac{P_T(X)}{P_S(X)}$ is intractable and during implementation this term is set to 1. Namely, the last line of Eq.(13) is approximately equal to

$$\begin{aligned} &\mathbb{E}_{X \sim \tilde{\mathcal{D}}_S} \left[\frac{P_T(X)}{P_S(X)} |h - f_S| \right] + \epsilon_T(f_S, f_T) \\ &= \epsilon_S(h) + \epsilon_T(f_S, f_T) \\ &\leq \epsilon_S(h) + \epsilon_S(f_S, f_T) + d_{\mathcal{H}}(\tilde{\mathcal{D}}_S, \tilde{\mathcal{D}}_T) \end{aligned} \quad (15)$$

Combining Eq.(14) and Eq.(15) we can get the error bound in Eq.(13) is upper bounded by

$$\epsilon_S(h) + d_{\mathcal{H}}(\tilde{\mathcal{D}}_S, \tilde{\mathcal{D}}_T) + \min\{\epsilon_S(f_S, f_T), \epsilon_T(f_S, f_T)\}, \quad (16)$$

which completes our proof.

A.5 Reformulation of the density ratio.

In this subsection, we first introduce some important definition of distributionally robust optimization (DRO) framework [7] and then reformulate the density ratio under some necessary assumptions. In DRO, the worst-case expected risk over a predefined family of distributions \mathcal{Q} (termed *uncertainty set*) is used to replace the expected risk on the unseen target distribution \mathcal{T} in ERM. Therefore, the objective is as follows,

$$\min_{\theta \in \Theta} \max_{q \in \mathcal{Q}} \mathbb{E}_{(x,y) \in q} [\ell(x, y; \theta)]. \quad (17)$$

Specifically, the uncertainty set \mathcal{Q} encodes the possible test distributions that we want our model to perform well on. If \mathcal{Q} contains \mathcal{T} , the DRO object can upper bound the expected risk under \mathcal{T} .

The construction of uncertainty set \mathcal{Q} is of vital importance. Here we reformulate the density ratio based on the KL-divergence ball constraint and other choices (*e.g.*, using moment constraint [9], *f*-divergence [24], Wasserstein/MMD ball [33, 34]) will lead to different reweighting methods. Given the KL upper bound (radius) η , denote the empirical distribution \mathcal{P} , we have the uncertainty set $\mathcal{Q} = \{Q : \text{KL}(Q||\mathcal{P}) \leq \eta\}$. The min-max problem in Eq.(17) can then be reformulated as

$$\min_{\theta \in \Theta} \max_{Q: \text{KL}(Q||\mathcal{P}) \leq \eta} \mathbb{E}_{(x,y) \in Q} [\ell(x, y; \theta)]. \quad (18)$$

Then we have the following theorem, which derives the optimal density ratio and converts the original problem to a reweighting version.

Theorem 2. (Modified from Section 2 in [15]) Assume the model family $\theta \in \Theta$ and \mathcal{Q} to be convex and compact. The loss ℓ is continuous and convex for all $x \in \mathcal{X}, y \in \mathcal{Y}$. Suppose empirical distribution \mathcal{P} has density $p(x, y)$. Then the inner maximum of Eq.(18) has a closed-form solution

$$q^*(x, y) = \frac{p(x, y)e^{\ell(x,y;\theta)/\tau^*}}{\mathbb{E}_{\mathcal{P}} [e^{\ell(x,y;\theta)/\tau^*}]}, \quad (19)$$

where τ^* satisfies $\mathbb{E}_{\mathcal{P}} \left[\frac{e^{\ell(x,y;\theta)/\tau^*}}{\mathbb{E}_{\mathcal{P}} [e^{\ell(x,y;\theta)/\tau^*}]} \left(\frac{\ell(x,y;\theta)}{\tau^*} - \log \mathbb{E}_{\mathcal{P}} [e^{\ell(x,y;\theta)/\tau^*}] \right) \right] = \eta$ and $q^*(x, y)$ is the optimal density of \mathcal{Q} . The min-max problem in Eq.(18) is then equivalent to

$$\min_{\theta \in \Theta, \tau > 0} \tau \log \mathbb{E}_{\mathcal{P}} [e^{\ell(x,y;\theta)/\tau}] + \eta\tau. \quad (20)$$

B Algorithms for Test-time Model Selection Strategies

C Dataset details

Colored MNIST [5] consists of digits in MNIST with different colors (either blue or red). The label is a noisy function of the digit and color. First, a preliminary label \bar{y} is assigned

Algorithm 1: Cosine Similarity Measurement (CSM).

Input: training data $\{\mathcal{D}_i\}_{i=1}^K$, test data \mathcal{D}_T , batch size N , learning rate η , training iterations T .
Initial: Classifiers $\{h_i\}_{i=1}^K$ with parameter $\{\theta_i^h\}_{i=1}^K$, encoder g with parameter θ^g .
//During Training
for $t = 1, \dots, T$ **do**
 $\{(x_i^k, y_i^k, d_k)_{i=1}^N \sim \mathcal{D}_i\}_{k=1}^K$ *//Data sampling, (data, label, domain label)*
 $\mathcal{L} = \sum_{k=1}^K \sum_{i=1}^N \ell(x_i^k, y_i^k; \theta^{g,t-1}, \theta_i^{h,t-1})$ *//Calculate the empirical loss*
 $\theta^{g,t} \leftarrow \text{SGD}(\mathcal{L}, \theta^{g,t-1}, \eta)$; $\{\theta_i^{h,t} \leftarrow \text{SGD}(\mathcal{L}, \theta_i^{h,t-1}, \eta)\}_{i=1}^K$ *//Update parameters*
end
//During Test
Calculate domain representations. $\{z_i = \frac{1}{|\mathcal{D}_i|} \sum_{x \in \mathcal{D}_i} g(x)\}_{i=1}^K$
for $x \in \mathcal{D}_T$ **do**
 $\{H_i = \text{cosine_similarity}(g(x), z_i)\}_{i=1}^K$ *//Calculate similarities.*
 $i^* = \arg \max \{H_i\}_{i=1}^K$ *//Similarity Maximization.*
 $y_t = \arg \max \bar{\mathbf{y}}^{i^*}$ *if not ensembling else* $\arg \max \sum_{k=1}^K \bar{\mathbf{y}}_k \frac{H_k^\gamma}{\sum_{i=1}^K H_i^\gamma}$ *//Result.*
end

Algorithm 2: Prediction Entropy Measurement (PEM).

Input: training data $\{\mathcal{D}_i\}_{i=1}^K$, test data \mathcal{D}_T , batch size N , learning rate η , training iterations T .
Initial: Classifiers $\{h_i\}_{i=1}^K$ with parameter $\{\theta_i^h\}_{i=1}^K$, encoder g with parameter θ^g .
//Training Process is the same as Algorithm 1
//During Test
for $x_t \in \mathcal{D}_T$ **do**
 $\{\bar{\mathbf{y}}^i := [y_1^i, \dots, y_c^i] = h_i \circ g(x_t)\}_{i=1}^K$ *//Make prediction by every classifier*
 $\{H_k = - \sum_{i=1}^c \frac{y_i^k}{\sum_{j=1}^c y_j^k} \log \frac{y_i^k}{\sum_{j=1}^c y_j^k}\}_{k=1}^K$ *//Calculate the prediction entropy.*
 $i^* = \arg \min \{H_i\}_{i=1}^K$ *//Prediction Entropy Minimization.*
 $y_t = \arg \max \bar{\mathbf{y}}^{i^*}$ *if not ensembling else* $\arg \max \sum_{k=1}^K \bar{\mathbf{y}}_k \frac{H_k^{-\gamma}}{\sum_{i=1}^K H_i^{-\gamma}}$ *//Result.*
 //The weighting term here is $H_i^{-\gamma}$ not H_i^γ in other two strategies, because result with small entropy should be assigned a large weight.
end

to images based on their digits, $\bar{y} = 0$ for digits 0-4 and $\bar{y} = 1$ for digits 5-9. The final label is obtained by flipping \bar{y} with probability 0.25. The color signal z of each sample is obtained by flipping y with probability p^d , where p^d is $\{0.2, 0.1, 0.9\}$ for three different

Algorithm 3: Neural Network Measurement (NNM).

Input: training data $\{\mathcal{D}_i\}_{i=1}^K$, test data \mathcal{D}_T , batch size N , learning rate η, η_d , training iterations T .

Initial: Classifiers $\{h_i\}_{i=1}^K$ with parameter $\{\theta_i^h\}_{i=1}^K$, encoder g with parameter θ^g , and domain discriminator h' with parameter θ^d .

//During Training

for $t = 1, \dots, T$ **do**

$\{(x_i^k, y_i^k, d_k)\}_{i=1}^N \sim \mathcal{D}_i\}_{k=1}^K$ //Data sampling, (data, label, domain label)

$\mathcal{L} = \sum_{k=1}^K \sum_{i=1}^N \ell(x_i^k, y_i^k; \theta^{g,t-1}, \theta_i^{h,t-1})$ //Calculate the empirical loss

$\theta^{g,t} \leftarrow \text{SGD}(\mathcal{L}, \theta^{g,t-1}, \eta)$; $\{\theta_i^{h,t} \leftarrow \text{SGD}(\mathcal{L}, \theta_i^{h,t-1}, \eta)\}_{i=1}^K$ //Update parameters

$\mathcal{L}_d = \sum_{k=1}^K \sum_{i=1}^N \ell(x_i^k, d_i^k; \theta^{g,t-1}, \theta_i^{d,t-1})$ //Calculate the domain discrimination loss.

$\theta^{d,t} \leftarrow \text{SGD}(\mathcal{L}_d, \theta^{d,t-1}, \eta_d)$; //Update discriminator

end

//During Test

for $x_t \in \mathcal{D}_T$ **do**

$[H_1, \dots, H_k] := \text{Softmax}(h'(x))$ //Discriminator prediction result.

$i^* = \arg \max\{H_i\}_{i=1}^K$ //Similarity Maximization.

$y_t = \arg \max \bar{\mathbf{y}}^{i^*}$ if not ensembling else $\arg \max \sum_{k=1}^K \bar{\mathbf{y}}_k \frac{H_k^\gamma}{\sum_{i=1}^K H_i^\gamma}$ //Result.

end

domains. Finally, images with $z = 1$ will be colored red and $z = 0$ will be colored blue. This dataset contains 70,000 examples of dimension (2, 28, 28) and 2 classes.

Rotated MNIST [12] consists of 10,000 digits in MNIST with different rotated angles where domain is determined by the degrees $d \in \{0, 15, 30, 45, 60, 75\}$.

PACS [19] includes 9,991 images with 7 classes $y \in \{\text{dog, elephant, giraffe, guitar, horse, house, person}\}$ from 4 domains $d \in \{\text{art, cartoons, photos, sketches}\}$.

VLCS [37] is composed of 10,729 images, 5 classes $y \in \{\text{bird, car, chair, dog, person}\}$ from domains $d \in \{\text{Caltech101, LabelMe, SUN09, VOC2007}\}$.

DomainNet [28] has six domains $d \in \{\text{clipart, infograph, painting, quickdraw, real, sketch}\}$. This dataset contains 586,575 examples of size (3, 224, 224) and 345 classes.

D Detailed Generalization Results

Table 8 shows the generalization performance on the ColoredMNIST of all baseline algorithms. No existing algorithm performs better than IRM, however, the propose DRM and its variants (incorporated with CORAL) beats these algorithms by a large margin. Generalization results on the Rotated MNIST (Table 9) show that the proposed DRM and its variants perform much better than baselines on challenging domains (domain $d = 0$ and domain $d = 5$) and then attain a better average generalization accuracy. For large

Algorithm	+90%	+80%	-90%	Avg
ERM [38]	71.8 ± 0.4	72.9 ± 0.1	28.7 ± 0.5	57.8
IRM [5]	72.0 ± 0.1	72.5 ± 0.3	58.5 ± 3.3	67.7
GDRO [30]	73.5 ± 0.3	73.0 ± 0.3	36.8 ± 2.8	61.1
Mixup [41]	72.5 ± 0.2	73.9 ± 0.4	28.6 ± 0.2	58.4
MLDG [18]	71.9 ± 0.3	73.5 ± 0.2	29.1 ± 0.9	58.2
CORAL [36]	71.1 ± 0.2	73.4 ± 0.2	31.1 ± 1.6	58.6
MMD [20]	69.0 ± 2.3	70.4 ± 1.6	50.6 ± 0.2	63.3
DANN [11]	72.4 ± 0.5	73.9 ± 0.5	24.9 ± 2.7	57.0
CDANN [21]	71.8 ± 0.5	72.9 ± 0.1	33.8 ± 6.4	59.5
MTL [8]	71.2 ± 0.2	73.5 ± 0.2	28.0 ± 0.6	57.6
SagNet [26]	72.1 ± 0.3	73.2 ± 0.3	29.4 ± 0.5	58.2
ARM [46]	84.9 ± 0.9	76.8 ± 0.6	27.9 ± 2.1	63.2
VREx [17]	72.8 ± 0.3	73.0 ± 0.3	55.2 ± 4.0	67.0
RSC [16]	72.0 ± 0.1	73.2 ± 0.1	30.2 ± 1.6	58.5
DRM	86.7 ± 2.4	80.6 ± 0.2	43.1 ± 7.5	70.1
+ CORAL	85.3 ± 2.3	80.7 ± 0.2	47.2 ± 3.6	71.1

Table 8: Domain generalization accuracies (%) on Colored MNIST.

benchmarks VLCS, PACS, and DomainNet, generalization results are shown in Table 10, Table 10, and Table 9 respectively. We observe that DRM outperforms existing algorithms on all these benchmarks, however, because CORAL performs not better than ERM in these benchmarks, incorporating CORAL with DRM is sometimes harmful.

E Additional Domain-classifier correlation matrixes

Figure 8 shows all Domain-classifier correlation matrixes on the Rotated MNIST, PACS, and VLCS datasets with different domains as the unseen target domain. The three characteristics mentioned in Sec. 4.3 still hold on to these matrixes. Besides, these Domain-classifier correlation matrixes reflect some dataset properties that cannot be observed by humans directly. As shown in Figure 7, domains in the VLCS dataset do not show significant visual differences, at least not as obvious as the rotation angle on Rotated MNIST or image style on PACS. However, the correlation matrixes attained by DRM still have distinct prediction entropy on different domain-classifier pairs.

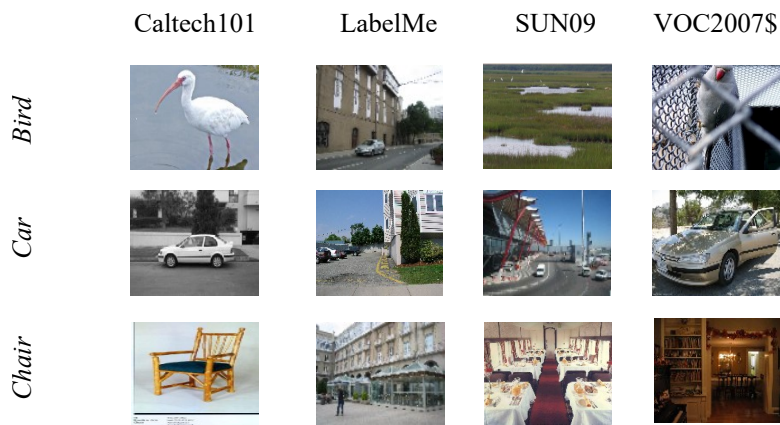


Figure 7: Samples on VLCS.

Rotated MNIST							
Algorithm	0	15	30	45	60	75	Avg
ERM [38]	95.3 ± 0.2	98.7 ± 0.1	98.9 ± 0.1	98.7 ± 0.2	98.9 ± 0.0	96.2 ± 0.2	97.8
IRM [5]	94.9 ± 0.6	98.7 ± 0.2	98.6 ± 0.1	98.6 ± 0.2	98.7 ± 0.1	95.2 ± 0.3	97.5
GDRO [30]	95.9 ± 0.1	99.0 ± 0.1	98.9 ± 0.1	98.8 ± 0.1	98.6 ± 0.1	96.3 ± 0.4	97.9
Mixup [41]	95.8 ± 0.3	98.7 ± 0.0	99.0 ± 0.1	98.8 ± 0.1	98.8 ± 0.1	96.6 ± 0.2	98.0
MLDG [18]	95.7 ± 0.2	98.9 ± 0.1	98.8 ± 0.1	98.9 ± 0.1	98.6 ± 0.1	95.8 ± 0.4	97.8
CORAL [36]	96.2 ± 0.2	98.8 ± 0.1	98.8 ± 0.1	98.8 ± 0.1	98.9 ± 0.1	96.4 ± 0.2	98.0
MMD [20]	96.1 ± 0.2	98.9 ± 0.0	99.0 ± 0.0	98.8 ± 0.0	98.9 ± 0.0	96.4 ± 0.2	98.0
DANN [11]	95.9 ± 0.1	98.9 ± 0.1	98.6 ± 0.2	98.7 ± 0.1	98.9 ± 0.0	96.3 ± 0.3	97.9
CDANN [21]	95.9 ± 0.2	98.8 ± 0.0	98.7 ± 0.1	98.9 ± 0.1	98.8 ± 0.1	96.1 ± 0.3	97.9
MTL [8]	96.1 ± 0.2	98.9 ± 0.0	99.0 ± 0.0	98.7 ± 0.1	99.0 ± 0.0	95.8 ± 0.3	97.9
SagNet [26]	95.9 ± 0.1	99.0 ± 0.1	98.9 ± 0.1	98.6 ± 0.1	98.8 ± 0.1	96.3 ± 0.1	97.9
ARM [46]	95.9 ± 0.4	99.0 ± 0.1	98.8 ± 0.1	98.9 ± 0.1	99.1 ± 0.1	96.7 ± 0.2	98.1
VREx [17]	95.5 ± 0.2	99.0 ± 0.0	98.7 ± 0.2	98.8 ± 0.1	98.8 ± 0.0	96.4 ± 0.0	97.9
RSC [16]	95.4 ± 0.1	98.6 ± 0.1	98.6 ± 0.1	98.9 ± 0.0	98.8 ± 0.1	95.4 ± 0.3	97.6
DRM	96.4 ± 0.2	98.4 ± 0.0	98.9 ± 0.2	99.0 ± 0.2	98.9 ± 0.2	96.8 ± 0.2	98.1
+ CORAL	96.9 ± 0.1	98.9 ± 0.2	98.9 ± 0.4	99.0 ± 0.1	98.9 ± 0.2	97.3 ± 0.3	98.3
DomainNet							
Algorithm	clip	info	paint	quick	real	sketch	Avg
ERM [38]	58.1 ± 0.3	18.8 ± 0.3	46.7 ± 0.3	12.2 ± 0.4	59.6 ± 0.1	49.8 ± 0.4	40.9
IRM [5]	48.5 ± 2.8	15.0 ± 1.5	38.3 ± 4.3	10.9 ± 0.5	48.2 ± 5.2	42.3 ± 3.1	33.9
GDRO [30]	47.2 ± 0.5	17.5 ± 0.4	33.8 ± 0.5	9.3 ± 0.3	51.6 ± 0.4	40.1 ± 0.6	33.3
Mixup [41]	55.7 ± 0.3	18.5 ± 0.5	44.3 ± 0.5	12.5 ± 0.4	55.8 ± 0.3	48.2 ± 0.5	39.2
MLDG [18]	59.1 ± 0.2	19.1 ± 0.3	45.8 ± 0.7	13.4 ± 0.3	59.6 ± 0.2	50.2 ± 0.4	41.2
CORAL [36]	59.2 ± 0.1	19.7 ± 0.2	46.6 ± 0.3	13.4 ± 0.4	59.8 ± 0.2	50.1 ± 0.6	41.5
MMD [20]	32.1 ± 13.3	11.0 ± 4.6	26.8 ± 11.3	8.7 ± 2.1	32.7 ± 13.8	28.9 ± 11.9	23.4
DANN [11]	53.1 ± 0.2	18.3 ± 0.1	44.2 ± 0.7	11.8 ± 0.1	55.5 ± 0.4	46.8 ± 0.6	38.3
CDANN [21]	54.6 ± 0.4	17.3 ± 0.1	43.7 ± 0.9	12.1 ± 0.7	56.2 ± 0.4	45.9 ± 0.5	38.3
MTL [8]	57.9 ± 0.5	18.5 ± 0.4	46.0 ± 0.1	12.5 ± 0.1	59.5 ± 0.3	49.2 ± 0.1	40.6
SagNet [26]	57.7 ± 0.3	19.0 ± 0.2	45.3 ± 0.3	12.7 ± 0.5	58.1 ± 0.5	48.8 ± 0.2	40.3
ARM [46]	49.7 ± 0.3	16.3 ± 0.5	40.9 ± 1.1	9.4 ± 0.1	53.4 ± 0.4	43.5 ± 0.4	35.5
VREx [17]	47.3 ± 3.5	16.0 ± 1.5	35.8 ± 4.6	10.9 ± 0.3	49.6 ± 4.9	42.0 ± 3.0	33.6
RSC [16]	55.0 ± 1.2	18.3 ± 0.5	44.4 ± 0.6	12.2 ± 0.2	55.7 ± 0.7	47.8 ± 0.9	38.9
DRM	59.2 ± 0.2	20.8 ± 0.3	47.2 ± 0.1	15.2 ± 0.2	60.9 ± 0.6	50.8 ± 0.5	42.4
+ CORAL	59.3 ± 0.1	22.0 ± 0.9	48.0 ± 0.9	15.1 ± 0.2	61.0 ± 0.0	50.9 ± 0.1	42.7

Table 9: Domain generalization accuracies (%) on Rotated MNIST and DomainNet.

Algorithm	VLCS				Avg
	C	L	S	V	
ERM [38]	97.6 ± 0.3	67.9 ± 0.7	70.9 ± 0.2	74.0 ± 0.6	77.6
IRM [5]	97.3 ± 0.2	66.7 ± 0.1	71.0 ± 2.3	72.8 ± 0.4	76.9
GDRO [30]	97.7 ± 0.2	65.9 ± 0.2	72.8 ± 0.8	73.4 ± 1.3	77.4
Mixup [41]	97.8 ± 0.4	67.2 ± 0.4	71.5 ± 0.2	75.7 ± 0.6	78.1
MLDG [18]	97.1 ± 0.5	66.6 ± 0.5	71.5 ± 0.1	75.0 ± 0.9	77.5
CORAL [36]	97.3 ± 0.2	67.5 ± 0.6	71.6 ± 0.6	74.5 ± 0.0	77.7
MMD [20]	98.8 ± 0.0	66.4 ± 0.4	70.8 ± 0.5	75.6 ± 0.4	77.9
DANN [11]	99.0 ± 0.2	66.3 ± 1.2	73.4 ± 1.4	80.1 ± 0.5	79.7
CDANN [21]	98.2 ± 0.1	68.8 ± 0.5	74.3 ± 0.6	78.1 ± 0.5	79.9
MTL [8]	97.9 ± 0.7	66.1 ± 0.7	72.0 ± 0.4	74.9 ± 1.1	77.7
SagNet [26]	97.4 ± 0.3	66.4 ± 0.4	71.6 ± 0.1	75.0 ± 0.8	77.6
ARM [46]	97.6 ± 0.6	66.5 ± 0.3	72.7 ± 0.6	74.4 ± 0.7	77.8
VREx [17]	98.4 ± 0.2	66.4 ± 0.7	72.8 ± 0.1	75.0 ± 1.4	78.1
RSC [16]	98.0 ± 0.4	67.2 ± 0.3	70.3 ± 1.3	75.6 ± 0.4	77.8
DRM	98.0 ± 0.4	69.1 ± 1.0	73.7 ± 0.8	79.2 ± 0.4	80.0
+ CORAL	96.6 ± 1.3	71.6 ± 1.1	69.1 ± 3.1	78.7 ± 0.4	79

Algorithm	PACS				Avg
	A	C	P	S	
ERM [38]	86.5 ± 1.0	81.3 ± 0.6	96.2 ± 0.3	82.7 ± 1.1	86.7
IRM [5]	84.2 ± 0.9	79.7 ± 1.5	95.9 ± 0.4	78.3 ± 2.1	84.5
GDRO [30]	87.5 ± 0.5	82.9 ± 0.6	97.1 ± 0.3	81.1 ± 1.2	87.1
Mixup [41]	87.5 ± 0.4	81.6 ± 0.7	97.4 ± 0.2	80.8 ± 0.9	86.8
MLDG [18]	87.0 ± 1.2	82.5 ± 0.9	96.7 ± 0.3	81.2 ± 0.6	86.8
CORAL [36]	86.6 ± 0.8	81.8 ± 0.9	97.1 ± 0.5	82.7 ± 0.6	87.1
MMD [20]	88.1 ± 0.8	82.6 ± 0.7	97.1 ± 0.5	81.2 ± 1.2	87.2
DANN [11]	87.0 ± 0.4	80.3 ± 0.6	96.8 ± 0.3	76.9 ± 1.1	85.2
CDANN [21]	87.7 ± 0.6	80.7 ± 1.2	97.3 ± 0.4	77.6 ± 1.5	85.8
MTL [8]	87.0 ± 0.2	82.7 ± 0.8	96.5 ± 0.7	80.5 ± 0.8	86.7
SagNet [26]	87.4 ± 0.5	81.2 ± 1.2	96.3 ± 0.8	80.7 ± 1.1	86.4
ARM [46]	85.0 ± 1.2	81.4 ± 0.2	95.9 ± 0.3	80.9 ± 0.5	85.8
VREx [17]	87.8 ± 1.2	81.8 ± 0.7	97.4 ± 0.2	82.1 ± 0.7	87.2
RSC [16]	86.0 ± 0.7	81.8 ± 0.9	96.8 ± 0.7	80.4 ± 0.5	86.2
DRM	87.4 ± 2.9	83.5 ± 0.8	96.0 ± 0.5	83.0 ± 0.7	87.5
+ CORAL	87.7 ± 1.7	81.7 ± 0.5	97.1 ± 0.2	83.1 ± 1.2	87.4

Table 10: Domain generalization accuracies (%) on VLCS and PACS.

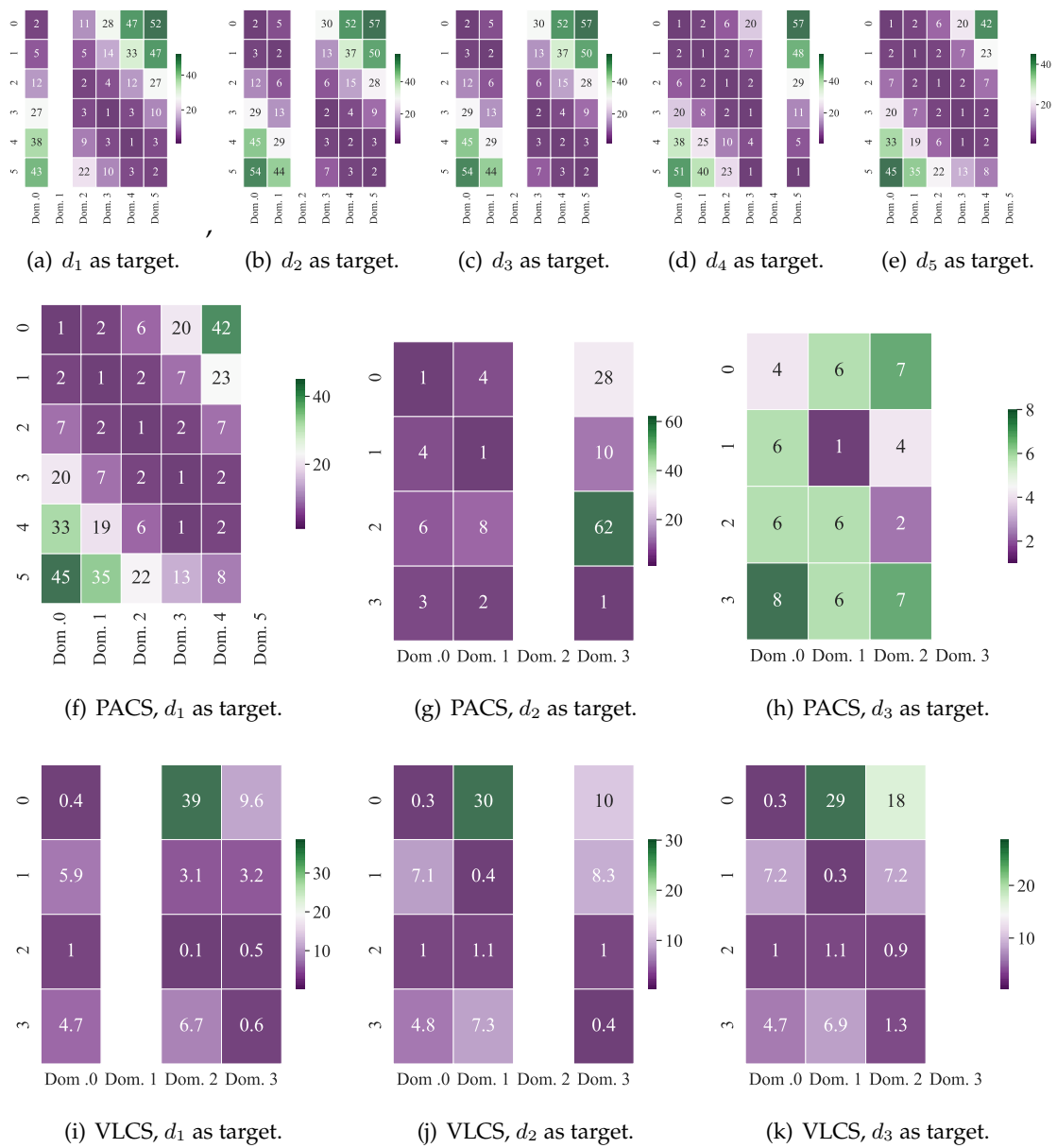


Figure 8: Domain-classifier correlation matrixes on (a,b,c,d,e) Rotated MNIST, (f,g,h) PACS, and (i,j,k) VLCS datasets.